

## Supplementary Information

### Design and synthesis of solution processable green fluorescent D- $\pi$ -A dyads for OLED applications

Shameel Thurakkal,<sup>a,b</sup> Krishnankutty S. Sanju,<sup>b,c</sup> Anjaly Soman,<sup>a,b</sup> K. N. Narayanan Unni,<sup>a,b</sup> Joshy Joseph<sup>\*a,b</sup> and Danaboyina Ramaiah<sup>\*b,d</sup>

<sup>a</sup>Photosciences and Photonics, Chemical Sciences and Technology Division, CSIR-National Institute for Interdisciplinary Science and Technology, Thiruvananthapuram-695 019

<sup>b</sup>Academy of Scientific and Innovative Research (AcSIR), CSIR-NIIST Campus, Thiruvananthapuram-695 019, Kerala, India.

<sup>c</sup>CSIR-Central Institute of Mining and Fuel Research, Dhanbad-826 015, Jharkhand, India.

<sup>d</sup>CSIR-North East Institute of Science & Technology, Jorhat-785 006, Assam, India.

E-mail: [rama@neist.res.in](mailto:rama@neist.res.in) or [d.ramaiah@gmail.com](mailto:d.ramaiah@gmail.com)

<b>SI No</b>	<b>Contents</b>	<b>Page</b>
1	Figures S1-S2 shows the $^1\text{H}$ NMR spectra of the dyads <b>1</b> and <b>2</b>	S3
2	Figures S3-S4 shows the $^1\text{H}$ NMR spectra of <i>p</i> -FOArBr and <i>m</i> -FOArBr	S4
3	Figures S5-S6 shows the $^{13}\text{C}$ NMR spectra of the dyads <b>1</b> and <b>2</b>	S5
4	Figures S7-S8 shows the $^{13}\text{C}$ NMR spectra of <i>p</i> -FOArBr and <i>m</i> -FOArBr	S6
5	Figures S9-S10 shows the ESI mass spectra of the dyads <b>1</b> and <b>2</b>	S7
6	Figures S11-S12 shows the ESI mass spectra <i>p</i> -FOArBr and <i>m</i> -FOArBr	S8
7	Figures S13 shows CIE chromaticity diagram of the dyads <b>1</b> and <b>2</b> corresponding to the emission spectra in (A) toluene and (B) film state	S9
8	Figures S14 shows ground state optimised geometries of the dyads <b>1</b> and <b>2</b>	S9
9	Figure S15 shows device structure, current density-voltage plot and CIE chromaticity diagram of the OLEDs	S10
10	Tables S1-S2 shows summary of absorption and emission properties of dyad <b>1</b> and <b>2</b> in various solvents	S11
11	Tables S3 shows comparison of properties of the present dyads with previously reported D-A type emitters	S12

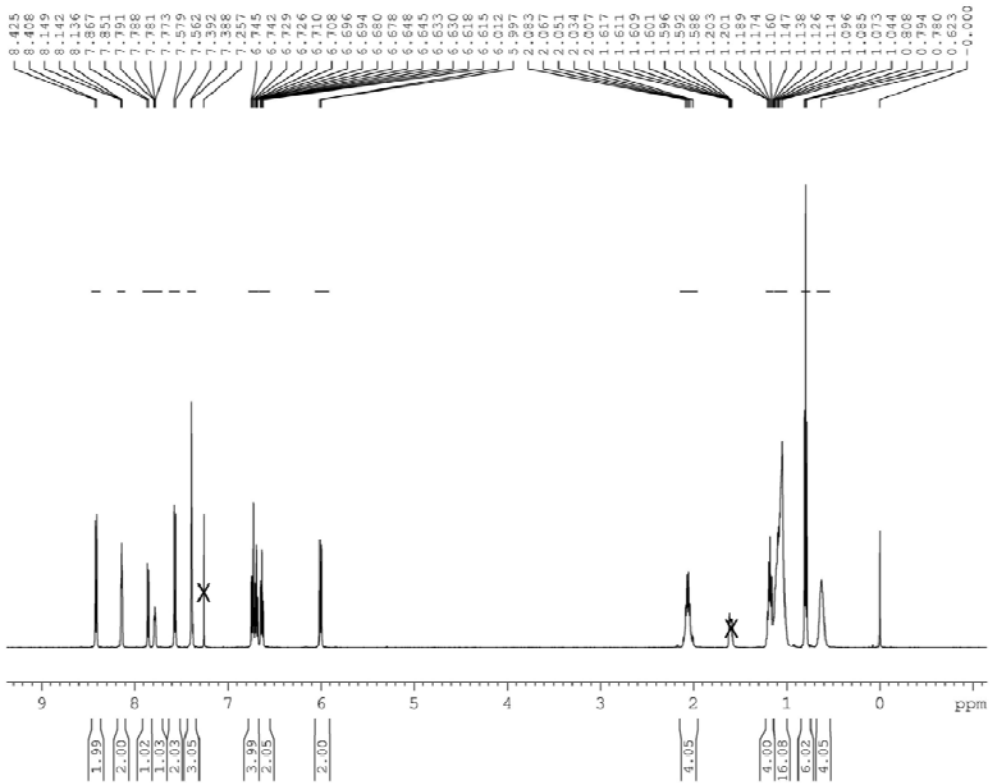


**Fig. S1**  $^1\text{H}$  NMR spectrum of the dyad **1** in  $\text{CDCl}_3$ .

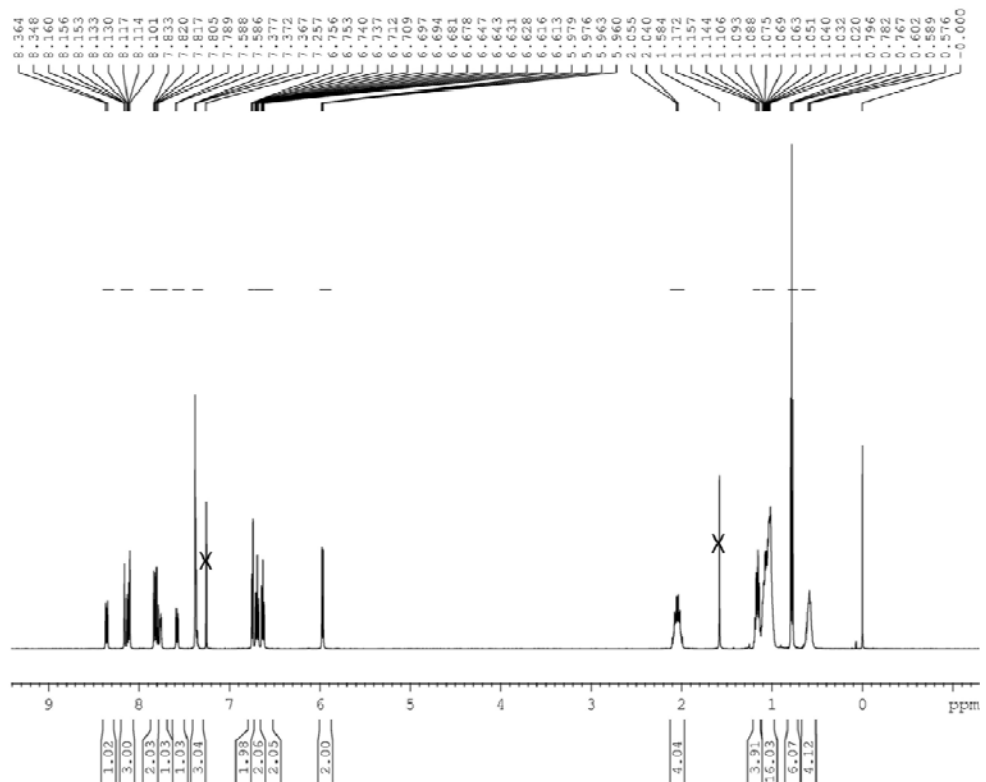


**Fig. S2**  $^1\text{H}$  NMR spectrum of the dyad **2** in  $\text{CDCl}_3$ .

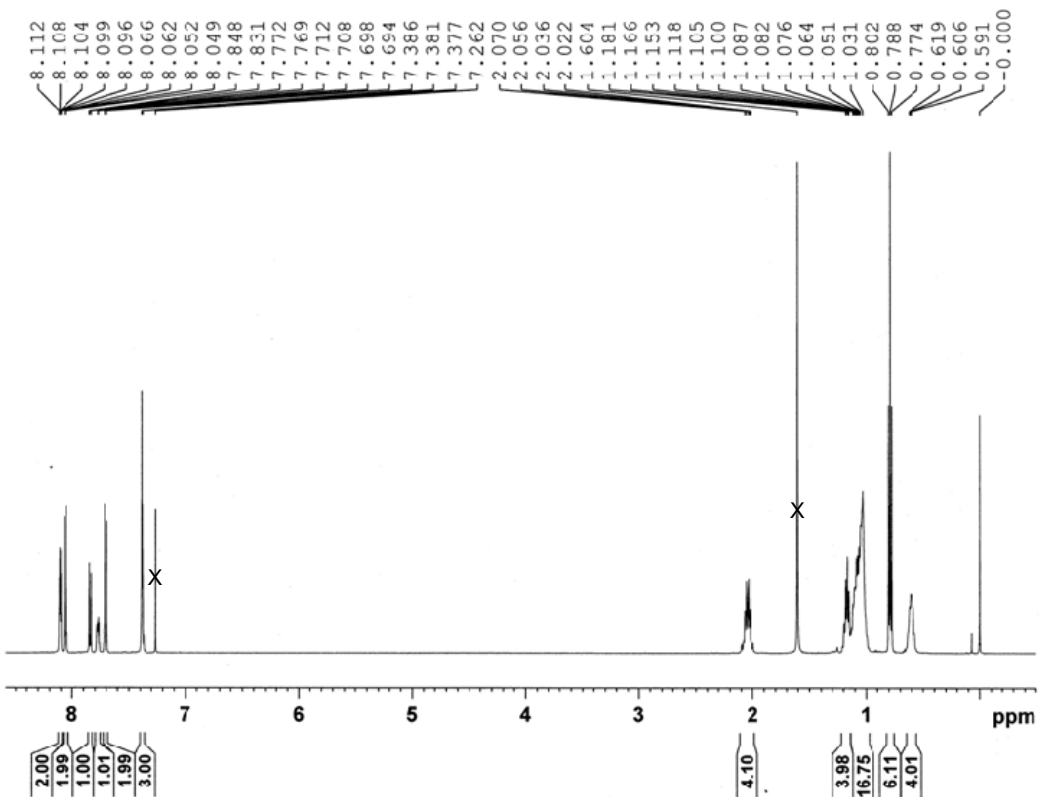


**Fig. S3**  $^1\text{H}$  NMR spectrum of *p*-FOArBr in  $\text{CDCl}_3$ .

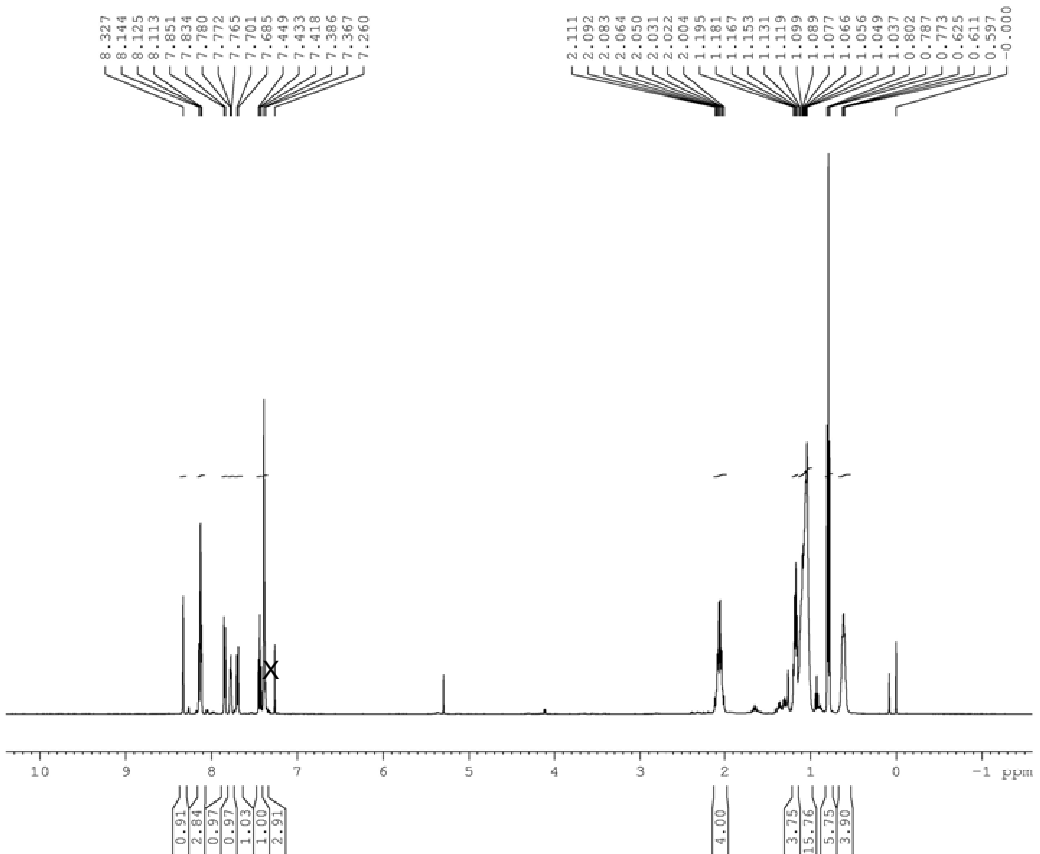


**Fig. S4**  $^1\text{H}$  NMR spectrum of *m*-FOArBr in  $\text{CDCl}_3$ .

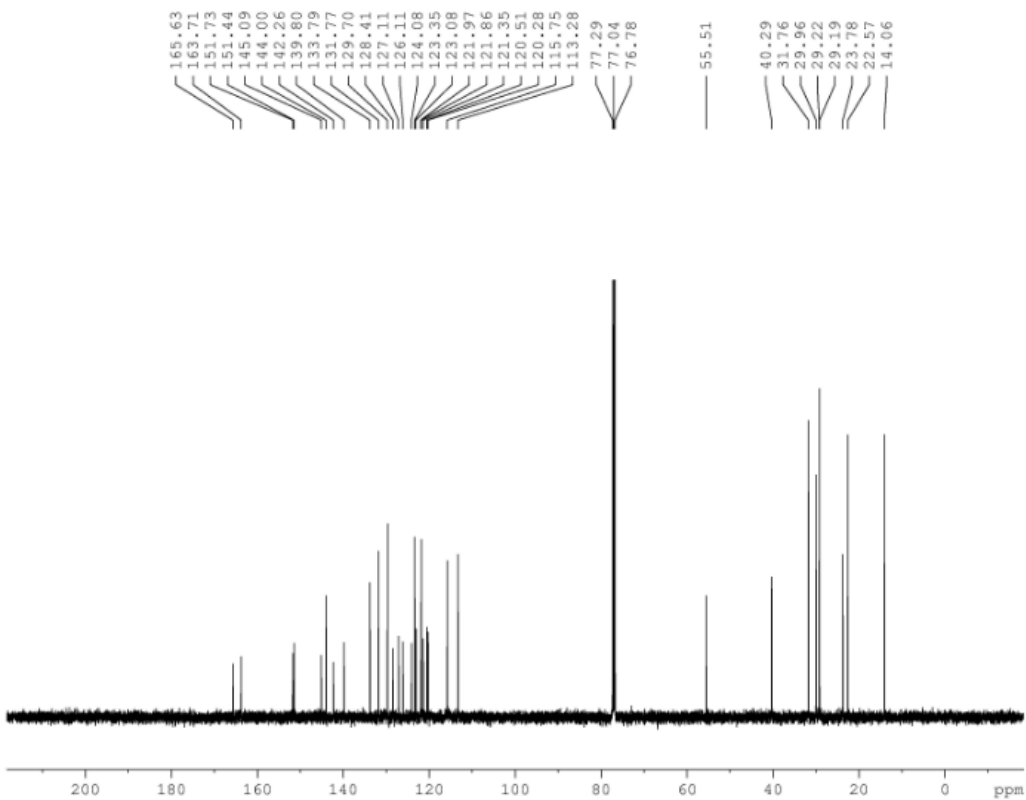


**Fig. S5**  $^{13}\text{C}$  NMR spectrum of the dyad **1** in  $\text{CDCl}_3$ .

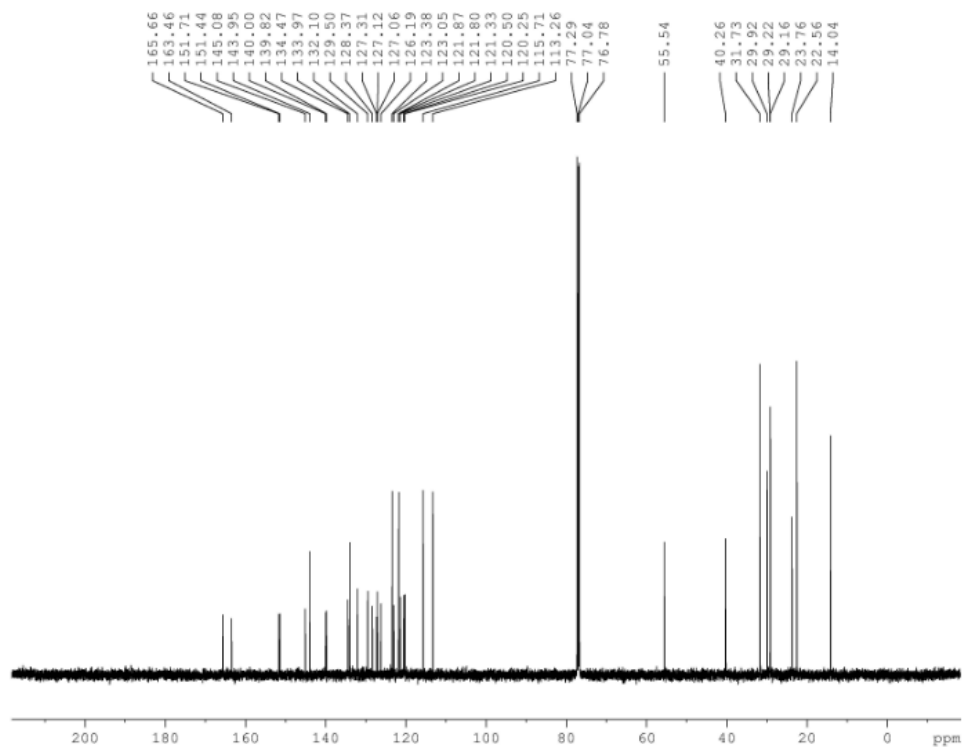


**Fig. S6**  $^{13}\text{C}$  NMR spectrum of the dyad **2** in  $\text{CDCl}_3$ .

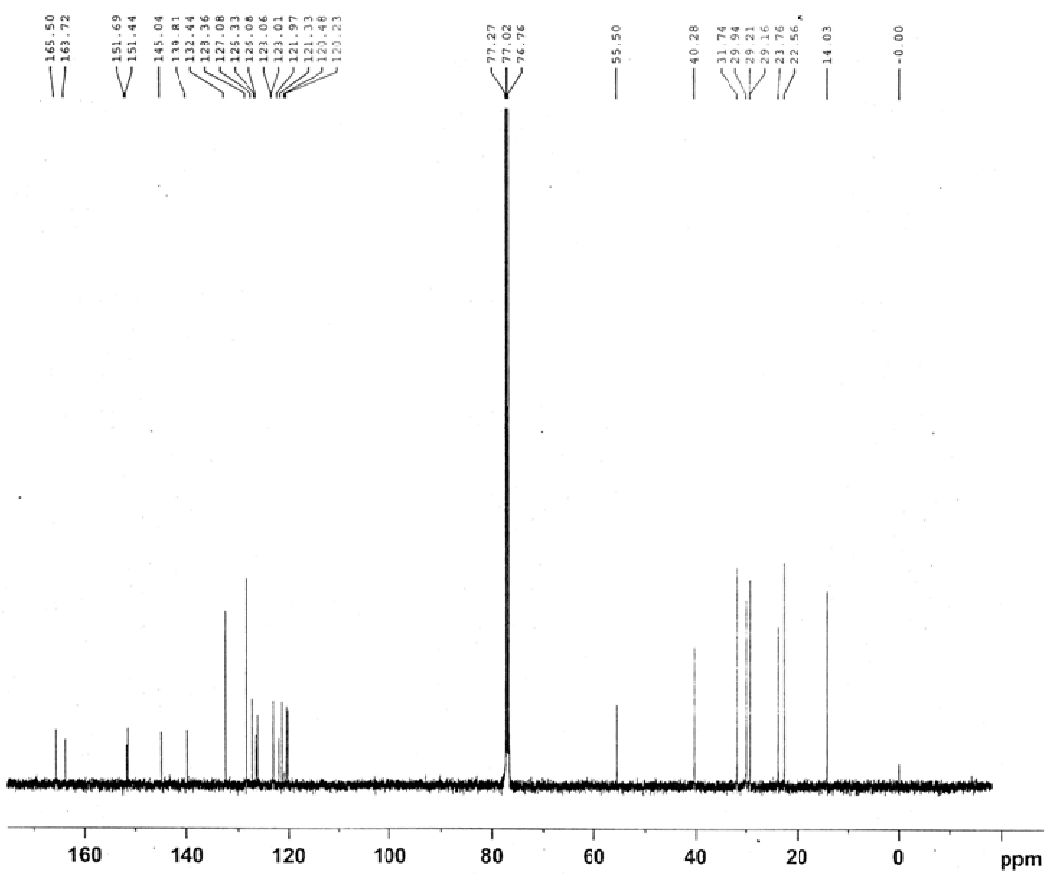


**Fig. S7**  $^{13}\text{C}$  NMR spectrum of *p*-FOArBr in  $\text{CDCl}_3$ .

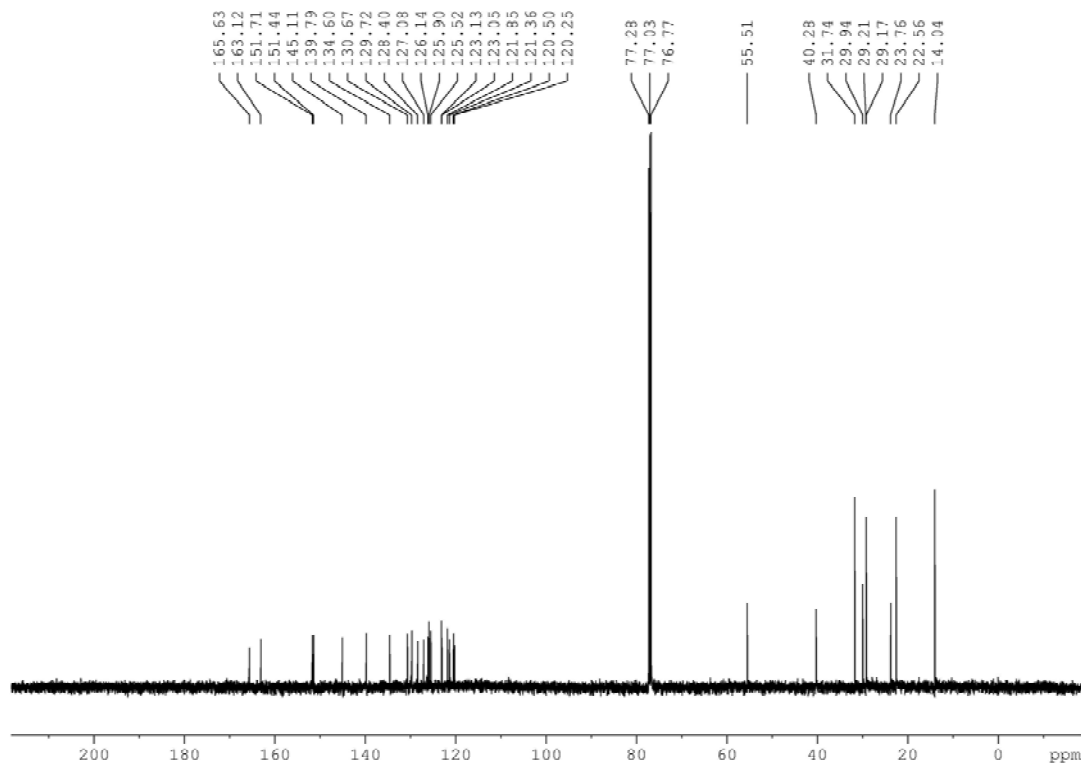


**Fig. S8**  $^{13}\text{C}$  NMR spectrum of *m*-FOArBr in  $\text{CDCl}_3$ .

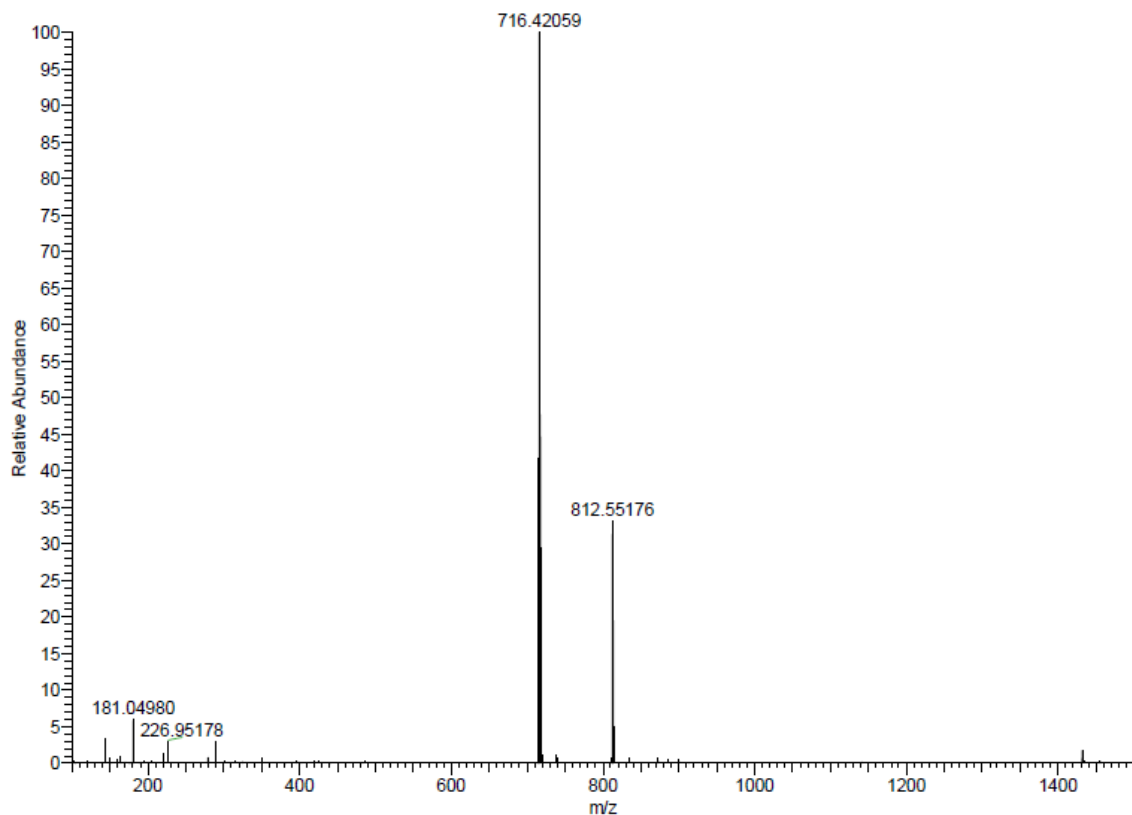


**Fig. S9** ESI mass spectrum of the dyad 1.

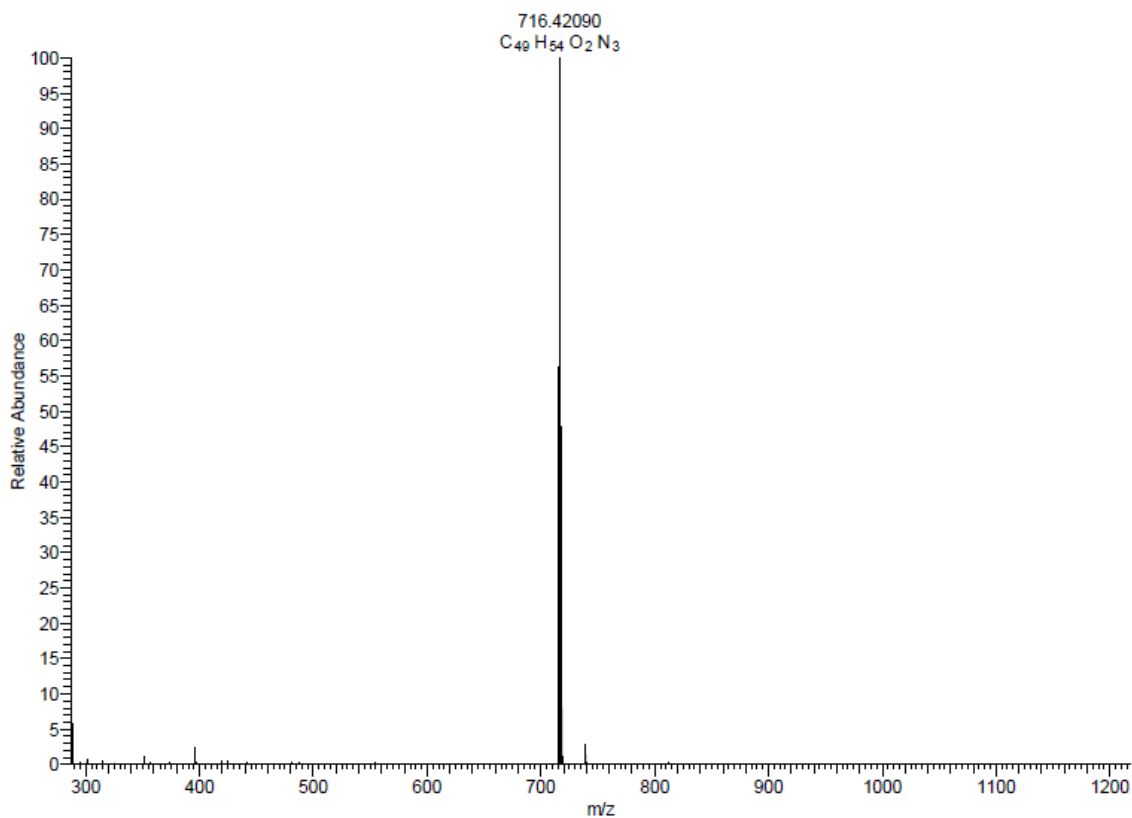


**Fig. S10** ESI mass spectrum of the dyad 2.

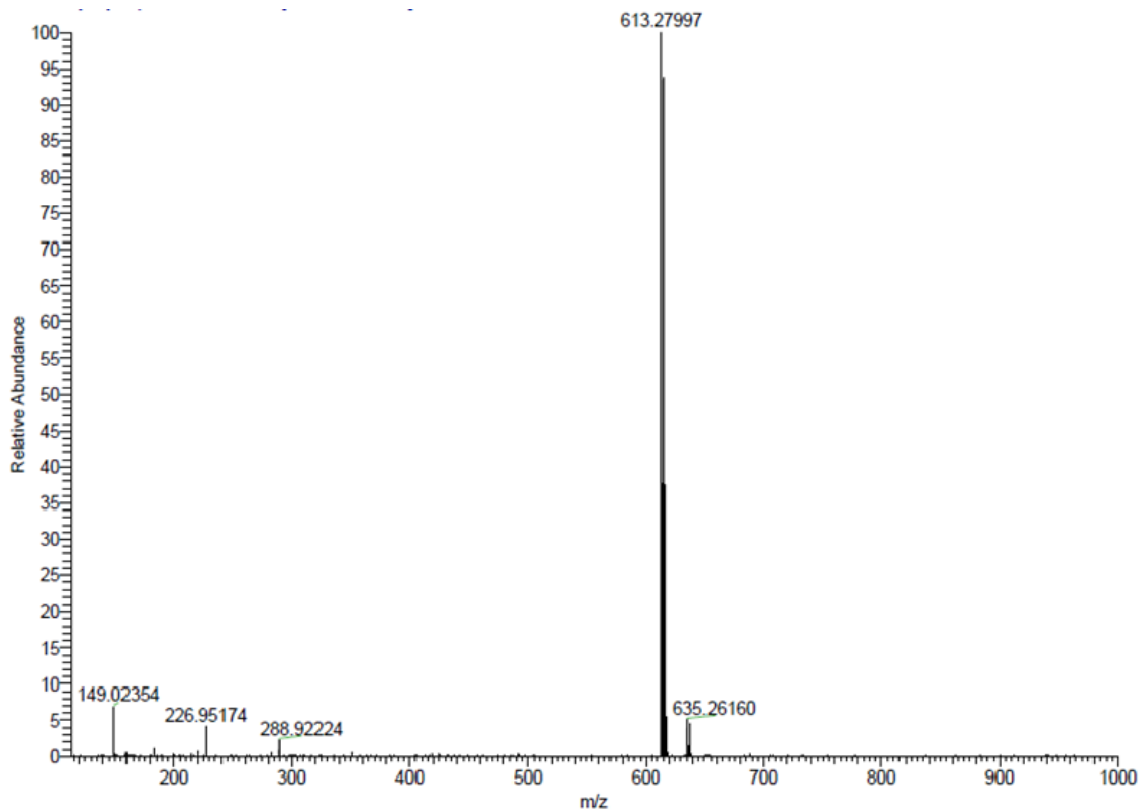


**Fig. S11** ESI mass spectrum of *p*-FOArBr.

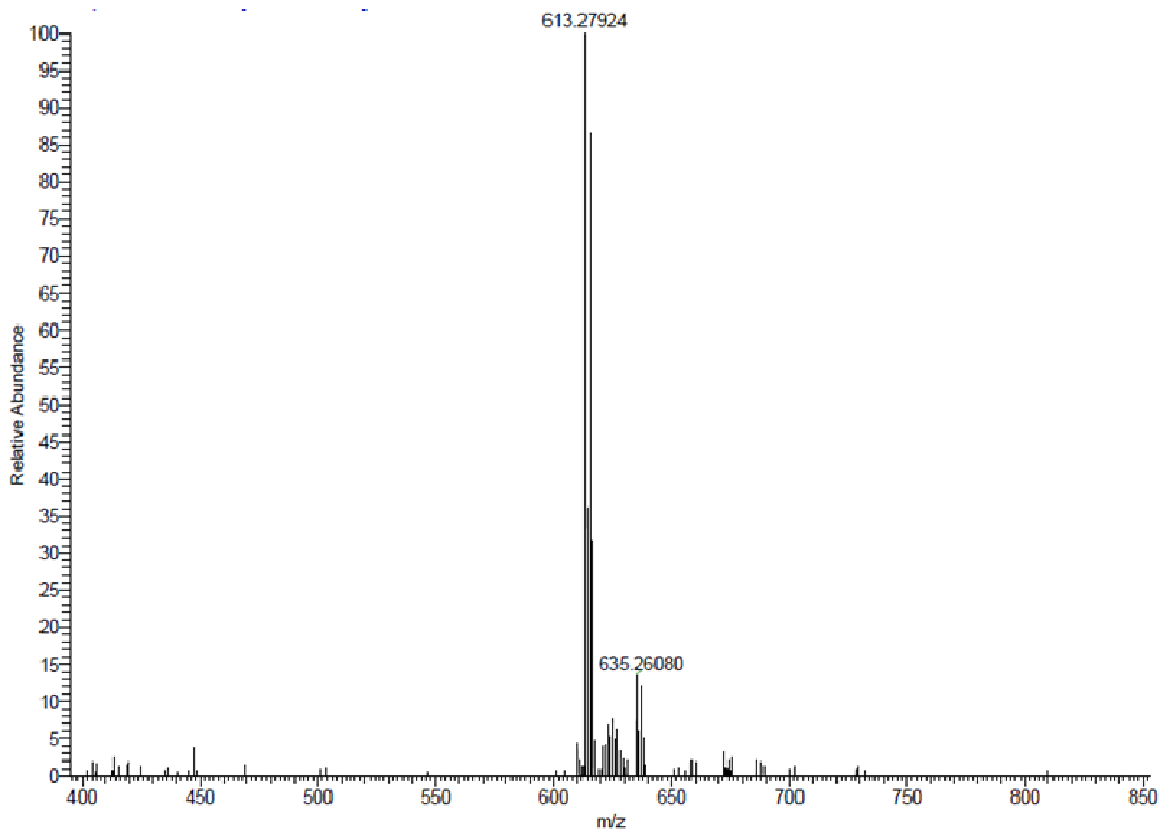


**Fig. S12** ESI mass spectrum of *m*-FOArBr.

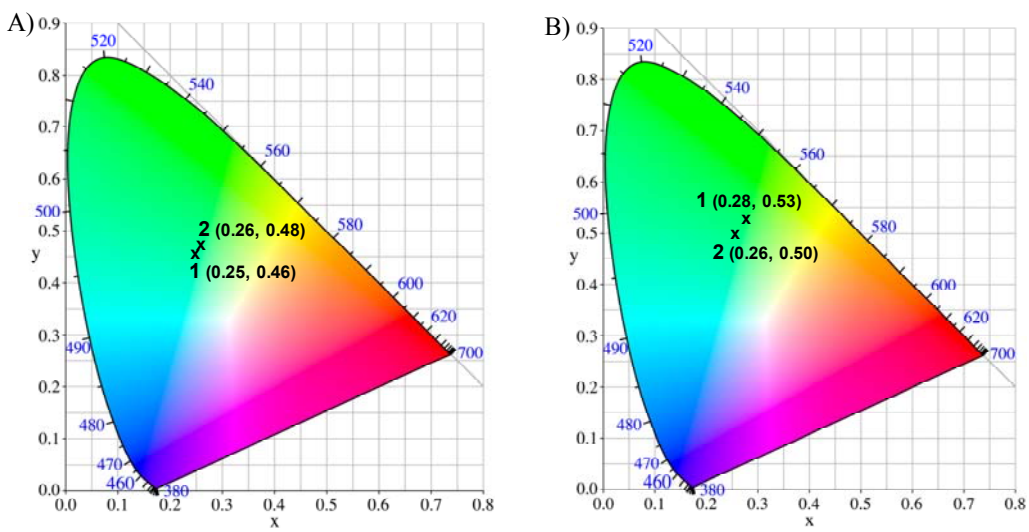


**Fig. S13** CIE chromaticity diagram of the dyads **1** and **2** corresponding to the emission spectra in (A) toluene and (B) thin film state.

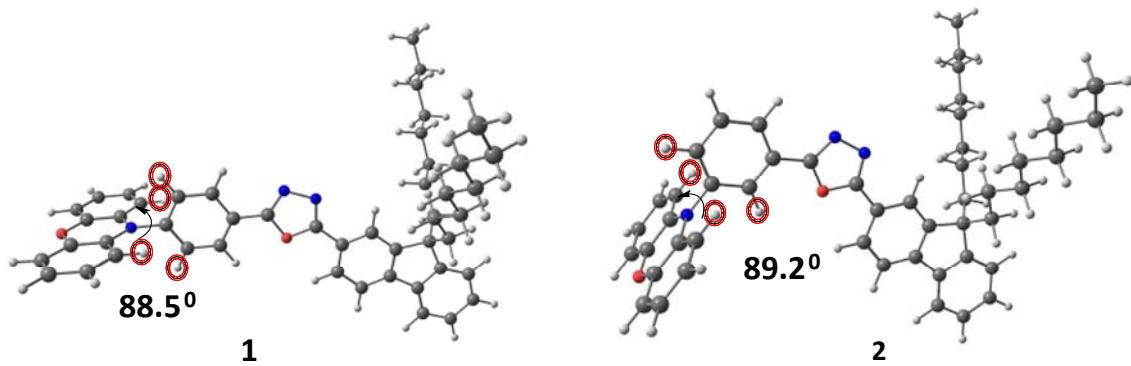


**Fig. S14** Ground state optimized geometries of the dyads **1** and **2**. The hydrogen atoms responsible for the twisted configuration are highlighted in red circles.

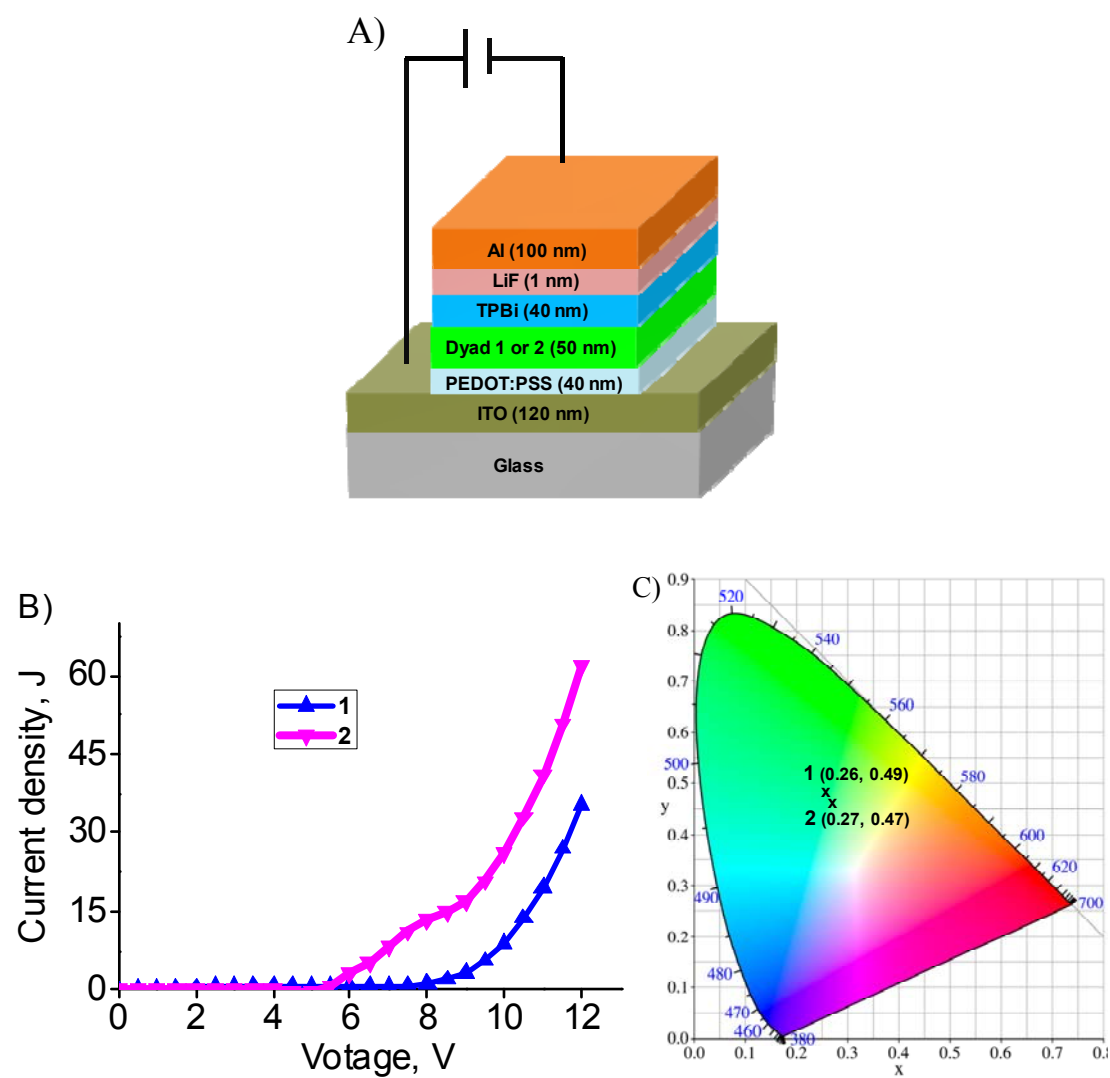


**Fig. S15** Device structure (A), current density-voltage plot (B) and CIE chromaticity diagram (C) of the OLEDs fabricated using the dyads **1** and **2**.

**Table S1** Absorption and emission properties of dyad **1** in different solvents.<sup>a</sup>

Solvents	$\epsilon$	n	$\Delta f$	$\lambda_a$ (nm)	$v_a$ (cm <sup>-1</sup> )	$\lambda_f$ (nm)	$v_f$ (cm <sup>-1</sup> )	$v_a \cdot v_f$ (cm <sup>-1</sup> )
Cyclohexane	2.02	1.43	0.005	327,390	30581.0	465	21505.4	9075.6
Toluene	2.38	1.49	0.013	328, 390	30487.8	505	19801.9	10685.8
DCM	9.10	1.42	0.220	328, 380	30487.8	562	17793.6	12694.2
Acetone	21.00	1.36	0.286	328, 373	30487.8	598	16722.4	13765.4
Acetonitrile	37.50	1.35	0.303	326, 372	30674.8	620	16129.0	14545.7

<sup>a</sup>Average of more than three independent experiments,  $\epsilon$ : dielectric constant, n: refractive index,  $\Delta f$ : solvent polarity parameter,  $\lambda_a$ : absorption wavelength,  $v_a$ : wave number corresponds to absorption maximum,  $\lambda_f$ : fluorescence wavelength,  $v_a$ : wave number corresponds to fluorescence maximum.

**Table S2** Absorption and emission properties of dyad **2** in different solvents.<sup>a</sup>

Solvents	$\Delta f$	$\lambda_{abs}$ (nm)	$v_a$ (cm <sup>-1</sup> )	$\lambda_f$ (nm)	$v_f$ (cm <sup>-1</sup> )	$v_a \cdot v_f$ (cm <sup>-1</sup> )
Cyclohexane	0.005	328,345	30487.8	465	21505.38	8982.4
Toluene	0.013	330, 345	30303.0	522	19157.09	11145.9
DCM	0.220	329, 343	30395.1	575	17391.30	13003.8
Acetone	0.286	328, 341	30487.8	610	16393.44	14094.4
Acetonitrile	0.303	326, 340	30674.8	625	16000.00	14674.8

<sup>a</sup>Average of more than three independent experiments,  $\Delta f$ : solvent polarity parameter,  $\lambda_a$ : absorption wavelength,  $v_a$ : wave number corresponds to absorption maximum,  $\lambda_f$ : fluorescence wavelength,  $v_a$ : wave number corresponds to fluorescence maximum.

**Table S3** Comparison of properties of the present dyads with previously reported D-A type emitters.

Sl. No	Publication	D-A Type	Thermal stability and device performance
1	Current Paper	Phenoxazine - Oxadiazole	Thermally stable up to 425 °C, excellent solution process-ability, film morphologies and un-doped OLED device performance based on dyad <b>1</b> : $L_{max} = 1751 \text{ cd/m}^2$ , $\lambda_{ems} = 504 \text{ nm}$ , CIE (0.26, 0.49).
2	<i>Photochem. Photobiol. Sci.</i> , 2014, <b>13</b> , 342 – 357	Anthracene - Oxadiazole	Thermally stable up to 364 °C and un-doped OLED device performance based on dyad <b>8A</b> : $L_{max} = 1284 \text{ cd/m}^2$ , $\lambda_{ems} = 485 \text{ nm}$ , $V_{onset} = 3 \text{ V}$ .
3	<i>New J. Chem.</i> , 2014, <b>38</b> , 2368 – 2378	Indolo[3,2-b]carbazole - Dimesitylboron	Thermally stable up to 210 °C and un-doped OLED device performance based on dyad <b>A</b> : $L_{max} = 5634 \text{ cd/m}^2$ ; $\lambda_{ems} = 472 \text{ nm}$ ; $V_{onset} = 6.1 \text{ V}$
4	<i>Chem. Asian J.</i> 2013, <b>8</b> , 2111 – 2124	Pyrene - Pyrenoimidazole	Thermally stable up to 500 °C and doped blue OLED device performance based on dyad <b>4c</b> : $L_{max} = 2980 \text{ cd/m}^2$ ; CIE (0.156, 0.135)
5	<i>Chem. Asian J.</i> 2010, <b>5</b> , 2093 – 2099	Triphenylamine - Benzimidazole	Thermally stable up to 531 °C and un-doped blue OLED device performance based on dyad <b>A</b> : $L_{max} = 4448 \text{ cd/m}^2$ ; $V_{onset} = 3.5 \text{ V}$ ; CIE (0.17, 0.07)
6	<i>J. Mater. Chem.</i> , 2009, <b>19</b> , 6172– 6184	Anthracene – Oxadiazole	Thermally stable up to 460 °C and un-doped OLED device performance based on dyad <b>5</b> : $L_{max} = 1996 \text{ cd/m}^2$ , $\lambda_{ems} = 535 \text{ nm}$ , $V_{onset} = 4 \text{ V}$ .